Peptides for *In Vivo* Target-Specific Cancer Imaging

G. Ferro-Flores[*,1], F. de M. Ramírez[2], L. Meléndez-Alafort[3] and C.L. Santos-Cuevas[1,4]

[1]*Department of Radioactive Materials. Instituto Nacional de Investigaciones Nucleares, Estado de México, Mexico*

[2]*Department of Chemistry. Instituto Nacional de Investigaciones Nucleares, Estado de México, Mexico*

[3]*Deparment of Pharmaceutical Science, Facoltà di Farmacia, Università di Padova, Italy*

[4]*Faculty of Medicine, Universidad Autónoma del Estado de México, Mexico*

Abstract: Molecular imaging comprises non-invasive monitoring of functional and spatiotemporal processes at molecular and cellular levels in living systems. Advanced imaging techniques can monitor such processes. Peptide receptors over-expressed in tumours can be targeted by peptides conjugated to radionuclides, near-infrared fluorochromes, metallic nanoparticles or quantum dots for target-specific cancer imaging.

Key Words: Peptides, molecular imaging, quantum-dots, nanoparticles.

INTRODUCTION

Regulatory peptide analogues represent a class of molecules developed for specific cancer targeting. In spite of having a relatively short history of about 2 decades, they are now receiving increasing interest, as they often are advantageously compared with immunotargeting using antibodies [1]. These peptides control and modulate the function of almost all key organs and metabolic processes and include neuropeptides which are present in the brain, gut peptide hormones, as well as peptides present in vascular (vasoactive peptides) and endocrine systems [2].

Regulatory peptide-receptors are proteins over-expressed in numerous human cancer cells. These receptors have been used as molecular targets for labelled peptides to localize tumours. The useful clinical results achieved during the last decade with somatostatin receptor-expressing neuroendocrine tumour imaging, have been useful for the study of other peptides to target alternative cancer-associated peptide receptors such as gastrin-releasing peptide, cholecystokinin, peptide ligands for integrin receptors or neurotensin. The improvement of peptide analogues allows specific clinical imaging and therapy of different tumour types, including breast, prostate, lung, intestine, pancreas and brain tumours [1,3,4]. Therefore, specific cancer targeting through selective peptides for diagnostic and therapeutic purposes is considered to be a promising strategy in oncology.

Molecular imaging comprises non-invasive monitoring of functional and spatiotemporal processes at molecular and cellular levels in humans and other living systems. Imaging techniques such as magnetic resonance imaging (MRI), single photon emission computed tomography (SPECT), positron emission tomography (PET) and optical fluorescence imaging (OI) have been used to monitor such processes. The present review affords an overview of the most outstanding *in vivo* peptides for cancer imaging using the different medical diagnostic techniques such as those mentioned above, which rely mostly on the use of radiopeptides and peptides conjugated to near-infrared fluorochromes, metallic nanoparticles or quantum dots (nanocrystals).

*Address correspondence to this author at the Departamento de Materiales Radiactivos, Instituto Nacional de Investigaciones Nucleares, Carretera México-Toluca S/N., La Marquesa, Ocoyoacac, Estado de México, C.P. 52750, México, Tel: + (52) (55)-53297200 ext. 3863; Fax. + (52) (55)-53297306; E-mail: ferro_flores@yahoo.com.mx, guillermina.ferro@inin.gob.mx

1. COMMON PEPTIDES USED AS RADIOLABELLED DIAGNOSTIC AGENTS

The term molecular imaging implies the *in vivo* characterization and measurement of biologic processes at cellular and molecular levels. In contrast to conventional diagnostic imaging, endeavours to probe the molecular abnormalities that are the basis of disease rather than to image the end effects of these molecular alterations [5].

Molecular biology, cell biology and imaging technology gave birth to molecular imaging as it is today. Three different non-invasive *in vivo* imaging technologies have been developed in parallel (MRI, OI, Nuclear Imaging), and peptide-specific targeting of a particular cell receptor can be imaged with a paramagnetic, fluorescent, or radionuclide-labelled probe. The convergence of these disciplines is the key of the molecular imaging success story and constitutes the source for further advances in the field.

Nuclear imaging is an established clinical molecular imaging modality that offers good sensitivity deep in tissue. Radiolabelled peptides (for PET and SPECT imaging) produce signals constantly through the decay of a radionuclide, whereas some probes produce signals only when they interact with its target (e.g., near-infrared fluorescent probes for optical imaging). Most radiolabelled peptides are administered at doses free of pharmacologic side effects (nonpharmacological nanogram levels) as compared with peptides for MRI and optical techniques that are usually dosed in mass levels (typically micrograms to milligrams).

1389-5575/10 $55.00+.00 **© 2010 Bentham Science Publishers Ltd.**

1.1 Somatostatin Analogues

Somatostatin is a cyclic peptide comprised of 14 amino acids and plays an important role in the secretion of hormones, such as growth hormone, insulin and glucagon. It is now recognized that there are five somatostatin receptor subtypes. Octreotide (OC) was developed as a somatostatin analogue for hypersecretion suppression to control the symptoms of neuroendocrine diseases. OC contains eight amino acids retaining an internal disulfide crosslink to constrain the geometry of the four essential amino acids, and is stable against enzymatic degradation *in vivo*. Pituitary adenomas and several neuroendocrine, tumours over-express somatostatin receptors such as: carcinoid, pancreas, pheochromocytomas, medullary thyroid carcinoma, paragangliomas, gastrinoma, glucagonoma, neuroblastoma, meningioma, insulinoma and small cell lung cancer. In somatostatin-based cancer imaging, a stable somatostatin analogue is linked to a bifunctional chelating agent that can bind radioactive elements such as, ^{111}In and ^{99m}Tc for SPECT or ^{18}F and ^{68}Ga for PET. Radiolabelled Tyr^3-OC (TOC) is currently used in the clinical practice as a stable complex to detect neuroendocrine tumours by molecular imaging in nuclear medicine [6-10]. ^{99m}Tc-Depreotide, a radiolabelled OC analogue developed in 1996 by Pearson *et al.* [11], has been recently approved for human use in USA and Europe because of its successful results in the diagnosis of solitary pulmonary nodules [12, 13]. A detailed list of 145 peptides labelled with ^{99m}Tc, ^{18}F, ^{68}Ga, ^{111}In, ^{64}Cu or ^{86}Y (29 to target somatostatin receptors) already investigated in clinical studies and those developed during the last five years (agonist and antagonist) has been recently reviewed [1,14].

1.2 Bombesin/Gastrin-Releasing Peptide Analogues

The small peptide bombesin (BN, 14 amino acids) was isolated from frog skin and it belongs to a large group of neuropeptides with many biological functions. The human equivalent is the gastrin-releasing peptide (GRP, 27 amino acids) and its receptors (GRP-r) are over-expressed in the tumour cell membrane. GRP differs from bombesin in only one of the 10 carboxy-terminal residues and this explains the similar biological activity of the two peptides. The strong, specific BN-GRP-r binding is the basis for labelling BN with radionuclides such as ^{68}Ga, ^{64}Cu, ^{18}F and ^{99m}Tc for nuclear imaging [15-22]. BN receptor subtype 2 (GRP receptor) is over-expressed in various human tumours including breast, prostate, small cell lung and pancreatic cancer, Fig. (**1**) [23-25]. Approximately 30 different radiolabelled peptides (agonist or antagonist) to target GRP-R have been recently reviewed [1,14,26].

1.3 Peptide Ligands for Cholecystokinin (CCK) and Gastrin receptors

Cholecystokinin (CCK) and gastrin act as neurotransmitters in the central nervous system, as regulators of various functions in the gastrointestinal tract, and as stimulatory

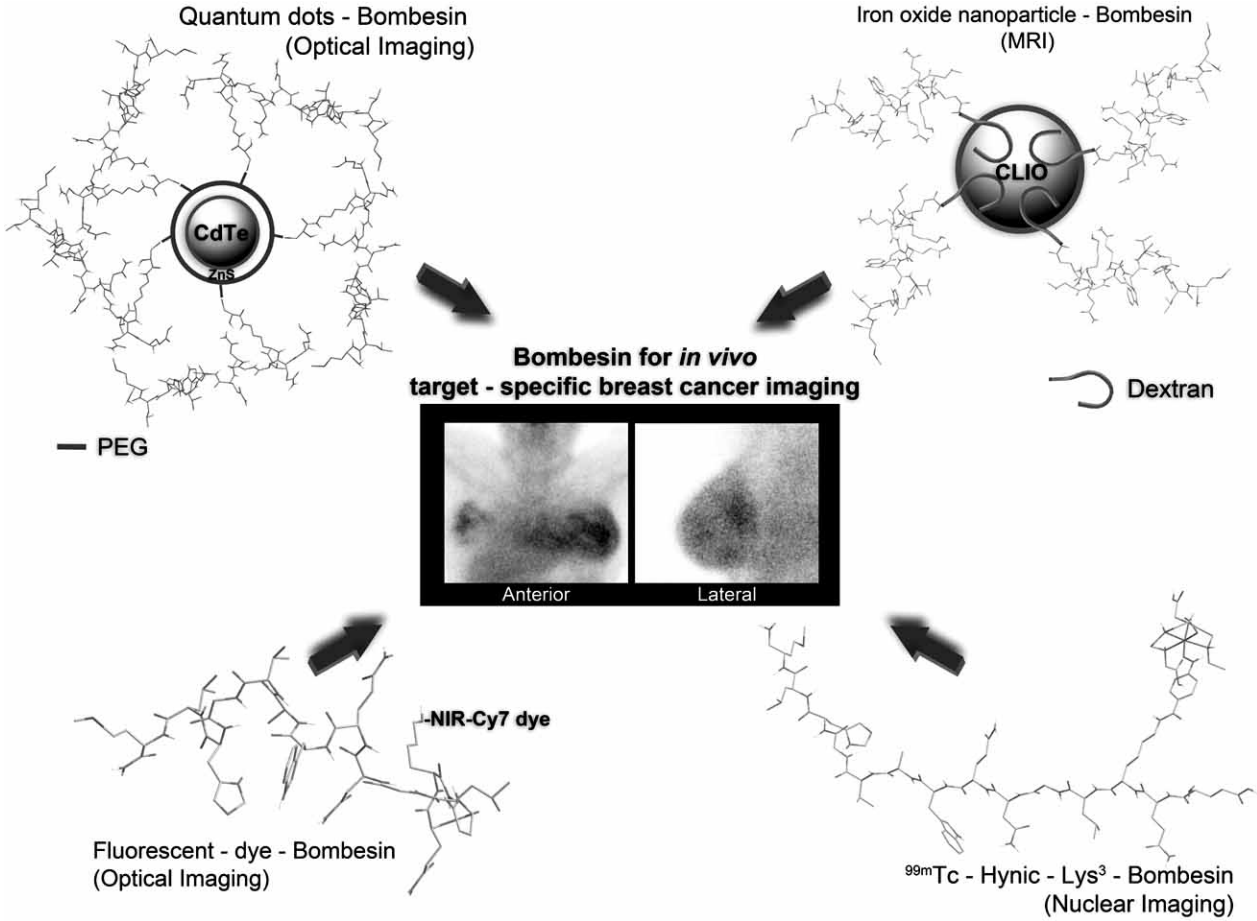

Fig. (1). Schematic illustration of the multiple modalities for *in vivo* target-specific cancer imaging with peptides conjugated to quatum dots, metallic nanoparticles, near-infrared fluorochromes or radionuclides.

growth factors in several tumours, such as colon and gastric cancers. They are structurally related in that they have the same C-terminal five amino acids (-Gly-Trp-Met-Asp-Phe-NH2), which is the active site for binding to cholecystokinin-2 (CCK-2) receptor. CCK-2 receptor protein has been identified in cell-membranes of medullary thyroid carcinomas (92 %), whereas it is absent in differentiated thyroid cancers. Specifically, ^{99m}Tc-labelled minigastrin has shown a high affinity for the CCK-2/gastrin-receptors *in vivo* [1,27,28]. Approximately 13 different peptides labelled with ^{99m}Tc or ^{111}In have been recently reported to target CCK-B receptors [14].

1.4 Peptide Ligands for Integrin αvβ3: Markers of Tumour Angiogenesis

"Angiogenesis represents the formation of new capillaries by cellular outgrowth from existing microvessels" [29]. Integrins are cell-adhesion receptors able to convert extracellular ligand binding into activation of intracellular processes (outside-in signalling) as well as employing intracellular processes to activate cellular responses (inside-out signalling). The alpha(v)beta(3) (αvβ3) integrin is involved in tumour induced angiogenesis and tumour metastasis. The high binding specificity to αvβ3 integrins of peptides containing Arg-Gly-Asp (RGD) residues has been used to radiolabel RGD peptides useful as tumour specific imaging agents.

A considerable number of synthetic peptides containing RGD have been developed. It has been found that constraining the RGD mobility in a cyclised pentapeptide increased the potency *in vitro*. These data suggest that the binding site in the αvβ3 receptor is limited.

Monomeric c-RGDyV (cyclic-Arg-Gly-Asp-D-Tyr-Val) peptide was first labelled in 1999 by Haubner *et al.* with ^{125}I [30]. This relatively lipophilic compound had rapid tumour washout and unfavourable hepatobiliary excretion. The resulting high liver and intestinal activity accumulation limited its further application. Glycosylation of the RGD peptide decreased the lipophilicity and, consequently, the hepatic uptake [31]. The same glycopeptides was then labelled with ^{18}F [32-33].

The peptide ligands for αvβ3 receptors mostly used in the labelling with ^{99m}Tc, ^{18}F or ^{68}Ga are c-RGDyK and c-RGDfK (cyclic-Arg-Gly-Asp-D-Phe-Lys) in both forms, as monomers or as dimers [34-40]. In these peptides the lysine side chain provides primary amine functionality for coupling bifunctional chelating agents. To improve targeting efficiency multimeric RGD systems have been design and more than 30 RGD derivatives labelled with ^{18}F, ^{64}Cu, ^{68}Ga or ^{99m}Tc have been developed [14, 41-43]. It is important to mention that RGD peptides do not belong to the regulatory peptide family, but are important since they can target neoangiogenic vessels through integrin receptors.

1.5 Peptide Ligands for Neurotensin Receptors

Neurotensin (NT) is a 14 amino acid linear peptide that is found in high concentration in the ileum and hypothalamus, and induces various physiologic effects such as hypotension, analgesia, gut contraction, and an increase of vascular permeability. Receptors of neurotensin are expressed in pancreatic and prostate cancer [1, 44]. ^{99m}Tc-labelled neuropeptide-Y (NPY) analogues are also useful for detecting sarcomas [45, 46].

Another receptors such as melanocortin-1 (MC1R), vasointestinal peptide (VPAC-1), glucagon-like-peptide-1 (GLP-1) and chemokine 4 (CXCR4) have also been targeted *in vivo* with radiolabelled peptides and recently discussed [14, 43].

1.6 Tat Penetrating Peptides

Targeted entry into cells is an increasingly important research area. Diagnoses and treatment of disease by novel methods would be greatly enhanced by efficiently transporting materials to living cell nuclei. Penetrating peptides (PPs) are attractive drug delivery tools. The PPs used in molecular imaging are mainly based on two peptides, HIV Tat peptide (TATp; RKKRRQRRR) and antennapedia homeodomain peptide (Antp or "penetrating"; RQIKIWFQNRRMKWKK) [47]. The HIV Tat-derived peptide is a small basic peptide called "trojan horse" because it has been successfully used to deliver a large variety of cargoes into cells such as nanoparticles, proteins, peptides and nucleic acids. The "transduction domain" or region conveying cell penetrating properties appears to be confined to a small stretch of basic amino acids with the sequence RKKRRQRRR and known as Tat(49-57) [47-50]. Hybrid radiopharmaceuticals, as for example ^{99m}Tc-N_2S_2-Tat(49-57)-Lys^3-Bombesin, have demonstrated a significant increasing cancer cell uptake and consequently image contrast of breast cancer tumours [51]. Tat peptides do not belong to the regulatory peptide family.

2. PEPTIDES FOR OPTICAL IMAGING

Nuclear imaging is limited by several factors such as time consuming data acquisition, expensive equipment, exposure to radioactivity, the need for highly skilled personnel [5]. Optical imaging offers real-time, nonradioactive, and, depending on the technique, high-resolution imaging of fluorophores embedded in diseased tissues [52]. Of the various optical imaging techniques investigated to date, near-infrared (NIR, 700-1000 nm wavelength) fluorescence-based imaging is of particular interest for non-invasive *in vivo* imaging because of the relatively low tissue absorption, scatter, and minimal autofluorescence of NIR light [53]. This is because haemoglobin (the primary absorber of visible light), water and lipids (the primary absorbers of infrared light) have their lowest absorption coefficients in the NIR region [54,55]. Deeper tissue areas are thus accessible for tomographic display of the optical signals. Advanced fluorescence imaging techniques, such as fluorescence molecular tomography (FMT) [56-63] and fluorescence reflectance imaging (FRI) [64-66], commonly employ NIR wavelengths for *in vivo* molecular imaging applications. Fluorescence imaging methods are generally superior in terms of sensitivity and ease of use [54]. However, NIR fluorescence imaging in small animals cannot be directly scaled up to *in vivo* imaging in patients due to the limited optical signal penetration depth ($\leq$ 7 mm by fluorescence resonance imaging and $\leq$ 20 cm by fluorescence molecular tomography) [54]. In clinical settings, fluorescence imaging is relevant for

tissues close to the surface of the skin and tissues accessible by endoscopy and intraoperative visua-lization [67].

2.1 Near-Infrared Fluorochromes

Organic fluorescent dyes are the most commonly used fluorochromes. Dyes such as fluorescein isothiocyanate (FITC) and carboxyfluorescein diacetatesuccinimidyl ester (CFSE) have been used for various biological applications, such as fluorescent-labelled antibodies and molecules that are used to stain cells or organelles [68]. However, they are prone to rapid photobleaching (fast photochemical destruction of a fluorophore by the light exposure) and, thus, are unsuitable for extended periods of bioimaging observations. Most organic dyes have a relatively broad emission spectrum. Emission/excitation wavelength is often affected by changes in local chemical environment (e.g., pH, interacting ions,etc.). Because of this, exogenously administered fluorochromes that fluoresce in the NIR region [60-71] such as cyanine (Cy) dyes, are now finding increasingly application in fluorescence imaging, but when the emitted light wavelength is beyond λ=850 nm their quantum yield is low (low brightness) with low photostability [72, 73] (Fig. **2**). However, the commercial available near-IR carboxyfluorescein (Near-IR CF^{TM} dyes Biotum, USA), with absorption and emission wavelengths between 650 and 800 nm, is reported to be significantly brighter and more stable than other commercial dyes of similar wavelength, Fig. (**2**). CF750 is so bright and can be excited at 633 nm (i.e., at the shoulder wavelength of the absorption maximum) but still emits stronger fluorescence at ~770 nm than APC-based tandem dyes, i.e. Cy7. It is possible to find in the near future interesting NIR fluorescence images using this new dye.

Fluorescence intensity of some cyanine dyes changes upon specific reaction with nitric oxide, which is an important signalling molecule involved in the regulation of a wide range of physiological and pathophysiological mechanisms, and many disorders [74].

In the particular case of peptides, novel NIR fluorescent arginine-glycine-aspartic acid (RGD) compounds with improved receptor binding affinity, cellular internalization, and other activities are being studied to improve the sensitivity and specificity of tumour targeting. The combination of the specificity of RGD peptide/integrin interaction with near-infrared fluorescence detection may be applied to non-invasive imaging of integrin expression and monitoring anti-integrin treatment efficacy providing near real-time measurements.

Chen *et al.* [75] showed that the Cy5.5-RGD conjugate exhibits affinity for αvβ3 integrin (IC(50) = 58.1 ± 5.6 nmol/L). *In vivo* imaging with a prototype three-dimensional small-animal imaging system visualized subcutaneous U87MG glioblastoma xenograft with a broad range of concentrations of fluorescent probe administered via the tail vein. Tumour uptake was blocked by unlabelled c(RGDyK) demonstrating the Cy5.5-RGD specificity [75]. Authors also synthesized Cy5.5-conjugated mono-, di-, and tetrameric RGD peptides to investigate the effect of multimerisation of RGD peptide on integrin avidity and tumour targeting efficacy. All three peptide-dye conjugates had integrin specific uptake both *in vitro* and *in vivo*. Among them, tetramer displayed the highest tumour uptake and tumour-to-normal tissue ratio from 0.5 to 4 h postinjection. Tumour-to-normal tissue ratio for Cy5.5-conjugated RGD monomer, dimer, and tetramer were found to be 3.18 ± 0.16, 2.98 ± 0.05, and 3.63 ± 0.09, respectively, at 4 h postinjection. These results suggested that Cy5.5-conjugated monomeric, dimeric, and tetrameric RGD peptides are all suitable for integrin expression imaging [76].

The αvβ3 expression has also been assessed in an orthotopic brain tumour model by using a three-dimensional optical imaging system (IVIS 200) after administration of monomeric Cy5.5-RGD. NIRF imaging showed the highest tumour uptake and tumour to normal brain tissue ratio at 2 h postinjection (2.64 ± 0.20). Tumour uptake of Cy5.5-RGD was effectively blocked by using unlabelled c(RGDyK) and

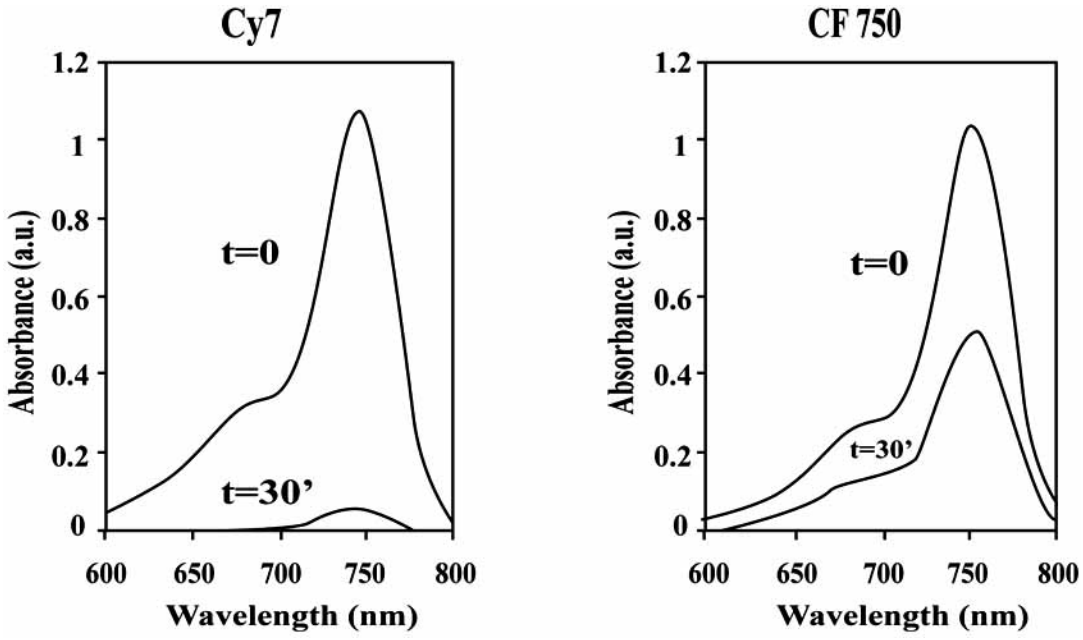

Fig. (2). Absorption spectra of Cy7 and CF750 NIR-dyes, before (t=0) and after (t=30 min) exposure to sunlight. (Biotum, USA).

injection of Cy5.5 dye alone showed nonspecific binding [77].

Wang *et al.* [78] worked with a cyanine labelled cyclic RGD pentapeptide. The tumour-to-background ratios for human Kaposi's sarcoma in mice injected with Cy5.5-c(KRGDf) and Cy5.5 were 5.5 and 1.5, respectively [78]. Gurfinkel *et al.* [79] obtained dynamic fluorescence images from a subcutaneous human Kaposi's sarcoma tumour model in mice immediately following the intravenous injection of Cy5.5-c(KRGDf). The fluorescence images, acquired via an intensified charge-coupled device detection system, were used in conjunction with a pharmacokinetic model to determine kinetic properties of target binding in the presence and absence of a competitive ligand (free c(KRGDf)). Results indicated that the conjugate dye behaves similarly in normal tissue to the free Cy5.5 while it possesses increased uptake in tumour tissue. Authors concluded that *in vivo* pharmacokinetic analysis based on dynamic optical imaging may be potentially useful in molecular medicine.

Mono-, di-, and tetrameric RGD peptides were synthesized and conjugated with Cy7 by Wu *et al.* [80]. The integrin specificity of these fluorescent probes was tested *in vitro* for receptor binding assay and fluorescence microscopy and *in vivo* for subcutaneous U87MG tumour targeting. The tetrameric Cy7-RGD peptide probe with the highest integrin affinity showed the highest tumour activity accumulation and strongest tumour-to-normal tissue contrast.

Waldeck *et al.* [81] reported that Cy5.5-RGD, combined with near-infrared optical imaging methods, allows the specific imaging of αvβ3 integrin expression on macrophages recruited to vascular lesions and may serve to estimate macrophage-bound inflammatory activity of atherosclerotic lesions.

The development of fluorescent molecules using dicarboxylic acid-containing carbocyanine fluorophore (cypate)-RGD with high and selective tumour uptake *in vivo* for optical tumour imaging in mice has also been reported [82, 83]. Such fluorescent molecules not only accelerate the screening of new compounds for lead discovery and optimization at cellular levels, but they are also advantageous in tracking, visualizing, and quantifying target specific fluorescent probes *in vivo* for distribution and metabolism studies. Recently, the evaluation of novel NIR fluorescent multimeric RGD systems based on the simplest RGD motif and cypate showed a remarkable increase in binding affinity respect to the monomer cypate-RGD-NH_2. *In vivo* non-invasive optical imaging showed that the compounds were retained in A549 human non-small-cell lung tumour tissue [84].

Red-region fluorescent dye doped silica nanoparticles (FSiNPs) have also been reported for molecular *in vivo* imaging. In these nanoparticles, cyanine derivative molecules are covalently bound to silica matrix to avoid the dye leaking out nanoparticles in bio-applications. Wu *et al.* [85] reported the targeting and optical imaging of MDA-MB-231 human breast cancer cells using RGD peptide-labelled FSiNPs. Tissue images demonstrated that the high αvβ3 expression level of the MDA-MB-231 tumours in nude mice was clearly visible and the tumour fluorescence reached maximum intensity at 1 h postinjection [85].

In 2007 Ma *et al.* developed the fluorescent probe Alexa Fluor 680-G-G-G-Bombesin[7-14]NH_2 and demonstrated the ability of this new conjugate to specifically target T-47D breast cancer tissue in mice by fluorescence images [86].

2.2 Quantum Dots

Quantum dots (QDs) or nanocrystals are fluorescent semiconductor nanoparticles (2-10 nm) with many unique optical properties including bright fluorescence, resistance to photobleaching, and a narrow emission bandwidth [87-90]. Their fluorescence emission wavelength can be continuously tuned from 400 nm to 2000 nm by changing both the particle size and chemical composition, at room temperature. Their quantum yields are as high as 85 %. The particles are generally made from hundreds to thousands of atoms (~200-10,000 atoms) of group II and VI elements (e.g. CdSe and CdTe) or group III and V elements (e.g. InP and InAs) [91]. Recent advances have allowed the precise control of particle size, shape and internal structure (core-shell, gradient alloy or homogenous alloy) [92-99]. As cadmium is potentially toxic, Gao *et al.* [100] developed a class of QD conjugates that contains an amphiphilic triblock copolymer for *in vivo* protection and multiple PEG molecules for improving biocompatibility and circulation. To make QDs more useful for *in vivo* imaging, they need to be effectively, specifically and reliably directed to a specific organ or disease site without alteration. Specific targeting can be achieved by attaching targeting molecules to the QD surface. Peptides and peptide analogues are suitable targeting ligands, as large numbers of these molecules can be linked to the surface of a single QD, Fig. (**1**) [67].

Water-soluble QDs may be cross-linked to peptides using standard bioconjugation protocols, such as the coupling of maleimide-activated QDs to thiol groups [101]. QDs can also act as sensors to detect the presence of biomolecules using intricate probe designs incorporating energy donors or acceptors. For example, QDs can be adapted to sense the presence of the sugar maltose by conjugating the maltose binding protein to the nanocrystal surface [102].

Recently, a detailed procedure for the preparation of QDs-RGD using commercially available PEG-coated QDs was reported by Cai and Chen [67]. A thiolated-RGD peptide was conjugated to QDs through 4-maleimidobutyric acid N-succinimidyl ester. Prior to *in vivo* imaging of human glioblastoma tumours which was successful in mice, competitive cell binding assay and live cell staining were carried out to confirm the successful attachment of the RGD peptides to the QD surface.

Shah *et al.* [103] used QDs-RGD for labelling of human mesenchymal stem cells (hMSCs) during self-replication and multilineage differentiations into osteogenic, chondrogenic, and adipogenic cells. Authors concluded that QDs-RGD is an effective probe for long-term labelling of stem cells.

Young and Rozengurt [104] demonstrated that QDs-bombesin conjugates can label the bombesin-preferring G protein-coupled receptors (GPCR) in living mice, suggesting that QDs technology can be adapted to monitor *in vivo* ligand binding to GPCRs.

QDs conjugated to the HIV Tat peptide, were quickly bound to cells and become internalized via endocytosis

[105]. Ruan *et al.* have recently used QDs-Tat as a model system to examine the cellular uptake and intracellular transport of nanoparticles in living cells [106]. The authors obtained dynamic fluorescence imaging. Results indicated that the peptide-conjugated QDs are internalized by macropinocytosis, in agreement with the recent work of Dowdy *et al.* [107]. It is interesting, that the internalized QDs-Tat are bound to the inner surface of vesicles and trapped in intracellular organelles. An important finding is that the QD-loaded vesicles are actively transported along microtubule tracks to an asymmetric perinuclear region called the microtubule organizing centre (MTOC) [108]. Furthermore, it was found that QDs-Tat strongly bind to cellular membrane structures. These results not only provide new insight into the mechanisms of Tat peptide-mediated delivery, but also are important for the development of nanoparticles probes for intracellular targeting and imaging.

2.3 Carbon Nanotubes

Single-walled carbon nanotubes (SWNTs) show physical properties that make them promising candidates for biological applications. However SWATs conjugated to peptides have only been studied in nuclear and photoacustic imaging. Liu *et al.* investigated the biodistribution of ^{64}Cu labelled SWNTs conjugated to PEG and RGD in mice with induced tumours by PET, ex vivo biodistribution and Raman spectroscopy. Results showed a high tumour conjugate accumulation attributed to the multivalent effect of the SWNTs [109]. The SWNT-RGD probe was also used as a photoacoustic molecular imaging agent in living mice [110].

2.4 Gold Nanoparticles

Gold nanoparticles (AuNPs) are inert and non-toxic, since Au(0) gold cores are taken up by human cells but do not cause acute cytotoxicity [111]. A second advantage is their easy synthesis [112]. There are two gold-nanoparticle properties that are most relevant: resistance to oxidation and plasmon resonance with light [113]. The plasmon resonance for ordinary gold nanospheres is at 520 nm, in the middle of the visible spectrum, but this can be red-shifted into the near infrared region (NIR) from 800 to 1200 nm. Further versatility is imparted by their readily functionalization with biological molecules to make them interact with a specific biological target. The conjugation of molecules to one AuNP is by means of the spontaneous reaction of a thiol (Cys) or a primary amine with the AuNP surface. Thiols are the most important type of stabilizing molecules for AuNPs of any size. It is an accepted assumption that the use of thiols leads to the formation of strong Au–S bonds [112, 114].

The fluorescence of AuNP rises from the surface plasmon resonance and can be enhanced, quenched or photobleached by the AuNP size, the nature of bounded cap to AuNP as well as the surrounding of the capped-AuNP. Ideally, the efficiency of the energy transfer to the AuNP from its organic cap only depends on the extent of the overlap of the cap band emission and the surface plasmon resonance band of the nanoparticle, which would be translated in a fluorescence resonance energy transfer (FRET) [115]. Fluorescence emission is very important in the study of AuNP conjugated to peptides since in general peptides contain aromatic residues which transfer their energy to the AuNP following the pathway: fluorescence level (peptide) to phosphorescence level (peptide) to surface plasmon resonance level (AuNP) and the absorbed light re-emitted, usually in the NIR range or close to- if the NIR fluorescence emission is not quenched or masked by the luminescence background in particular, in tissues.

Surujpaul *et al.* [115] prepared a stable multifunctional system of gold nanoparticles (AuNP) conjugated to [Tyr^3]Octreotide (TOC) peptide which was characterized by TEM, UV–Vis, infrared and fluorescence spectroscopy. AuNP and AuNP-TOC fluorescence emission spectra were obtained both in solution and in murine AR42J-tumour tissues. The fluorescence analyses in tissue revealed the recognition of the AuNP-TOC conjugate by the neuroendocrine tumour because of the lower energy position of the fluorescence resonance (692 nm) with respect to that of the AuNP in the same tumour tissue (684 nm). The emission band observed in the near infrared region (692 nm) opens the possibility for using AuNP-TOC in bioimaging. More than 500 TOC peptides can be bound to one 20 nm AuNP.

De La Fuente *et al.* have successfully prepared AuNPs functionalized with the Tat protein-derived peptide sequence GRKKRRQRRR in order to transport the NPs to the cell nucleus [116], and AuNP-RGD for possible phototherapeutic applications [117].

3. IRON OXIDE NANOPARTICLES CONJUGATED TO PEPTIDES FOR MRI

The quest for more potent and selective tumour-targeted diagnostic and therapeutic agents, and the widespread interest in nanotechnology have led to recent proposals that targeted nanoparticle-based pharmaceuticals might be designed to fit this need [118]. Nanoparticles offer two key advantages as targeted agents: nanoparticle geometry consisting of a core, typically with thousands of detectable atoms (iron and gold) and a coating, typically consisting of targeting peptides, antibodies or any molecule with biological activity. Nanoparticles produce multivalent effects due to multiple simultaneous interactions between the surface of the nanoparticle and the surface of the cell, whereas signals in nuclear imaging are the result of biological properties of single radiolabelled peptides.

The MRI technique is a non-invasive imaging modality capable of providing high resolution anatomical images. Basically, it uses the tissue contrast that is generated from the nuclear magnetic resonance (NMR) signals received from hydrogen nuclei located in different physiological environments in living systems. MRI can be expanded through the use of magnetic nanoparticles which improve the differentiation between malignant and healthy tissue. Iron oxide nanoparticles have magnetic properties and have been extensively investigated for biomedical applications due to their excellent biocompatibility and easy of synthesis [119-125]. The main requirement for MRI is the efficient capture of the magnetic nanoparticles by the cell and, when a cell is sufficiently loaded with magnetic material, MRI can also be used for cell tracking [126-127].

Recently, dextran coated superparamagnetic iron oxide nanoparticles (CLIO) labelled with Cy5.5 were conjugated to the 13- C-terminal amino acids of bombesin, which can bind to any of three receptors, the NMB receptor (BB1), the GRP receptor (BB2), or the orphan bombesin binding receptor BB3, showing the Bombesin-CLIO(Cy5.5) ability to visualize tumours in a model of pancreatic ductal adenocarcinoma by MRI [128]. Cy5.5 was included in the probe to assess presence of bombesin receptors by the fluorescein hapten visualization method.

Montet *et al.* [118] prepared cRGD-CLIO(Cy5.5) nanoparticles and evaluated the BT-20 human breast carcinoma cell integrin expression, nanoparticle pharmacokinetics and tumour vascularisation. Results indicated that magneto-fluorescent RGD nanoparticles were targeted to αvβ3-expressing tumour cells *in vivo* and were detectable by fluorescence reflectance imaging, fluorescence molecular tomography, and magnetic resonance imaging. Factors permitting the imaging of tumour integrins included the vascularised nature of the BT-20 tumour, the long nanoparticle blood half-life (180 min), and the ability of nanoparticles to slowly escape from the vasculature.

Surface modification of superparamagnetic contrast agents with the HIV-1 Tat peptide is an effective technique for intracellular magnetic labelling, because the conjugation of the Tat peptide to nanoparticles facilitates their cellular uptake [129]. Ultrasmall superparamagnetic iron oxide (USPIO) nanoparticles have been conjugated to the HIV Tat peptide to label CD4+ T cells. The number of Tat peptide molecules per nanoparticle was estimated to be from 15 to 45. Uptake in CD4+ T cells was determined using inductively coupled plasma optical emission spectrometry to measure iron content. Iron was detected in cells when USPIO-Tat nanoparticles were used, but no uptake was observed when unconjugated USPIO nanoparticles were used. Furthermore, it was demonstrated that labelled CD4+ T cells retained their proliferative and regulatory function *in vitro* and, similarly, no differences were observed in their transmigratory behaviour. The imaging potential of this contrast agent for MRI was evaluated, and USPIO-Tat provided effective contrast enhancement *in vitro*, while the unlabelled cells did not yield any contrast [130].

Another study in the same field addressed the feasibility of using MRI to monitor T cells *in vivo*. CLIO–Tat nanoparticles were conjugated to cells and results indicated that labelling of T cells with more than 8000 ng/ml of magnetic nanoparticles did not affect activation, proliferation or upregulation functions. A group of six B6 mice were injected intravenously with a suspension of T cells loaded with 8000 ng/mL of CLIO–Tat. Changes in spleen image intensity caused by the agent were measured by MRI, thereby proving that these particles can be used to analyze T-cell distribution events *in vivo* [131, 132].

Superparamagnetic nanoparticles of maghemite (γ-Fe2O3) have been encapsulated with an Arg-containing cell-penetrating peptide (RRRRRRRRCK–FITC). The FITC was conjugated to observe the intracellular translocation of magnetic nanoparticles into human mesenchymal stem cells, and cellular internalization was examined using a confocal laser scanning microscope (CLSM). Nanoparticles were effectively adsorbed onto the membrane of stem cells. Cell incubation with NP–peptide conjugates did not show significant cytotoxicity up to 200 μg/ml of IONP concentrations [133].

4. MULTIMODAL TECHNIQUES FOR MOLECULAR IMAGING

Molecular imaging represents the future of diagnostic imaging: it evolves from both anatomic and functional imaging as well as advances in genomics, cell and molecular biology, chemistry, and physics. Different imaging techniques are, in general, complementary rather than competitive. Dual-labelled targeting imaging agents, allow cross validation and direct comparison for example between nuclear (the goldstandard) and fluorescence optical image, or MRI and fluorescence, or trimodal nuclear- MRI-fluorescence.

For example, SPECT and PET provide functional information but lack the anatomical information. Computer tomography (CT) is a tomographic imaging technique that uses external X-ray source to produce 3-dimensional anatomic image data. The SPECT/CT and PET/CT systems, currently used in the clinical practice, combine a gammacamara and an integrated X-ray transmission system mounted on the same gantry [134, 135]. The advantage of SPECT/CT or PET/CT is the ability to acquire an anatomic image with CT and a functional image with SPECT or PET sequentially.

In the same direction, a dual-modality PET/NIR fluorescent peptide has been recently reported by Cai *et al.* [136]. A QD with an amine-functionalized surface was modified with RGD (90 peptides per QD) and 1,4,7,10-tetraaza-cyclododecane-N,N',N'',N'''-tetraacetic acid (DOTA) chelators for integrin αvβ3-targeted PET/NIRF imaging. PET/NIRF imaging, tissue homogenate fluorescence measurement, and immunofluorescence staining were performed with U87MG human glioblastoma tumour-bearing mice to quantify the ^{64}Cu-DOTA-QD-RGD uptake in tumour and major organs. Excellent linear correlation was obtained between the results measured by *in vivo* PET imaging and those measured by *ex vivo* NIRF imaging and tissue homogenate fluorescence. Histologic examination revealed that ^{64}Cu-DOTA-QD-RGD targets primarily the tumour vasculature through a RGD-integrin interaction, with little extravasation. Authors concluded that this dual-function probe has significantly reduced potential toxicity and overcomes the tissue penetration limitation of optical imaging, requisite for quantitative targeted imaging in deep tissue [136].

Fluorescent molecular tomographic (FMT) imaging can monitor molecular function in living animals using specific fluorescent probes. However, macroscopic imaging methods such as FMT generally exhibit low anatomical details. To overcome this, McCann *et al.* [137] reported a quantitative technique to image both structure and function by combining FMT and MRI. Authors demonstrated that FMT/MR imaging can produce three-dimensional, multimodal images of living mouse brains indispensable to serial monitoring of tumour morphology and protease activity. Combined FMT/MR tumour imaging provides a unique *in vivo* diagnostic parameter, which reflects histological changes in

tumours and is significantly altered for example by systemic chemotherapy. Combined FMT/MR imaging of fluorescent molecular probes could be valuable for brain tumour drug development and other neurological and somatic imaging applications [137].

The synthesis and *in vivo* characterization of an ^{18}F-CLIO was reported by Devaraj *et al*. [138]. This particle consists of cross-linked dextran molecules held together in core-shell formation by a superparamagnetic iron oxide core and functionalized with the radionuclide ^{18}F in high yield via "click" chemistry. Such nanoparticles could accurately detect lymph nodes (LNs), which are critical for assessing cancer metastasis. *In vivo* PET/MRI images could clearly identify small (~1 mm) LNs along with precise anatomical information.

NIR fluorescence has the potential to provide rapid, inexpensive, and nonradioactive population-based screening for breast cancer. Bhushan *et al*. [139] developed a system for detection of breast cancer microcalcifications using a dual-modality SPECT/NIR fluorescent probe.

Two or more different peptides can be bound to one AuNP. In our group we have obtained radiolabelled gold nanoparticles conjugated to two different peptides, one to be used as a bifunctional chelating agent to link the radionuclide and the other one as regulatory peptide analogue: ^{99m}Tc-GGC-AuNP-bombesin. This system could be useful for imaging breast cancer (data not published).

5. SUMMARY AND CONCLUSIONS

Labelled regulatory peptides, as well as RGD and Tat peptides, have far-reaching potential for the study of cellular processes at the single-molecule level, high-resolution cellular imaging, long-term *in vivo* observation of cell tracking, tumour targeting, and specific cancer diagnostic. Medical imaging modalities such as MRI, SPECT and PET can identify tumours non-invasively, but they do not provide a visual guide during surgery. Nanoparticle probes can endow imaging techniques with enhanced signal, sensitivity and better spatial resolution. For example, the development of magnetic or radioactive QD-peptides could give a visual guide during surgery.

Several molecular imaging strategies using multicomponent nanoparticles conjugated to peptides for multimodal imaging techniques are poised for rapid clinical application. Major areas of research are focused on development of molecular, functional and genetic imaging tools, aided by new information technology and image fusion/integration capabilities. Undoubtedly, multimodal imaging techniques using target-specific peptides will enhance the ability to accurately diagnose and evaluate the efficacy of different cancer therapies.

REFERENCES

[1] Reubi, J.C.; Maecke, H.R. Peptide-based probes for cancer imaging. *J. Nucl. Med.*, **2008**, *49*, 1735-38.

[2] Reubi, J.C.; Waser, B. Concomitant expression of several peptide receptors in neuroendocrine tumours: molecular basis for in vivo multireceptor tumour targeting. *Eur. J. Nucl. Med*., **2003**, *30*, 781-93.

[3] Ferro-Flores, G.; Arteaga de Murphy, C.; Melendez-Alafort, L. Third generation radiopharmaceuticals for imaging and targeted therapy. *Curr. Pharm. Anal*., **2006,** *2*, 339-52.

[4] de Visser, M.; Verwijnen, S.M.; de Jong, M. Update: improvement strategies for peptide receptor scintigraphy and radionuclide therapy. *Cancer Biother. Radiopharm*., **2008**, *23*, 137-57.

[5] Weissleder, R.; Mahmood, U. Molecular imaging. *Radiology*, **2001,** *219*, 316-33.

[6] Decristoforo, C.; Meléndez-Alafort, L.; Sosabowski, J.K.; Mather, S.J. ^{99m}Tc-HYNIC-[Tyr3]-Octreotide for imaging somatostatin-receptor-positive tumors: preclinical evaluation and comparison with ^{111}In-octreotide. *J. Nucl. Med.*, **2000,** *41*, 1114-19.

[7] Plachcinska, A.; Mikolajczak, R.; Maecke, H.R.; Mlodkowska, E.; Kunert-Radek, J.; Michalski, A.; Rzeszutek, K.; Kozak, J.; Kusmierek, J. Clinical usefulness of 99mTc-EDDA/HYNIC-TOC scintigraphy in oncological diagnostics: a preliminary communication. *Eur. J. Nucl. Med. Mol. Imaging*, **2003,** *30*, 1402-06.

[8] Plachcinska, A.; Mikolajczak, R.; Maecke, H.R.; Michalski, A.; Rzeszutek, K.; Kozak, J.; Kusmierek, J. ^{99m}Tc-EDDA/HYNIC-TOC scintigraphy in the differential diagnosis of solitary pulmonary nodules. *Eur. J. Nucl. Med. Mol. Imaging*, **2004**, *31*, 1005-10.

[9] Gonzalez-Vazquez, A.; Ferro-Flores, G.; Arteaga de Murphy, C.; Gutierrez-Garcia, Z. Biokinetics and dosimetry in patients of 99mTc-EDDA/HYNIC-Tyr3-octreotide prepared from lyophilized kits. *Appl. Radiat. Isot.*, **2006**, *64*, 792-97.

[10] Czepczynski, R.; Parisella, M.G.; Kosowicz, J.; Mikolajczak, R.; Ziemnicka, K.; Gryczynska, M.; Sowinski, J.; Signore, A. Somatostatin receptor scintigraphy using 99mTc-EDDA/HYNIC-TOC in patients with medullary thyroid carcinoma. *Eur. J. Nucl. Med. Mol. Imaging*, **2007**, *34*, 1635-45.

[11] Pearson, D.A.; Lister-James, J.; McBride, W.J.; Wilson, D.; Martel, L.J.; Civitello, E.R.; Taylor, J.E.; Moyer, B.R.; Dean, R.T. Somatostatin receptor-binding peptides labelled with technetium-99m: chemistry and initial biological studies. *J. Med. Chem.*,**1996**, *39*, 1361-71.

[12] Blum, J.; Handmaker, H.; Lister-James, J.; Rinne, N. A multicenter trial with a somatostatin analogue ^{99m}Tc-depreotide in the evaluation of solitary pulmonary nodules. *Chest*, **2000**, *117*, 1232-38.

[13] Plachcinska, A.; Mikoajczak, R.; Kozak, J.; Rzeszutek, K.; Kumierek, J. Comparative analysis of ^{99m}Tc-depreotide and ^{99m}Tc-EDDA/HYNIC-TOC thorax scintigrams acquired for the purpose of differential diagnosis of solitary pulmonary nodules. *Nucl. Med. Rev*., **2006**, *9*, 24-9.

[14] Scottelius, M.; Wester, H.-J. Molecular imaging targeting peptide receptors. *Methods*, **2009**, *48*, 161-77.

[15] La Bella, R.; Garcia-Garayoa, E.; Langer, M.; Bläuenstein, P.; Beck-Sickinger, A.G.; Schubiger, P.A. *In vitro* and *in vivo* evaluation of a ^{99m}Tc(I)-labeled bombesin analogue for imaging of gastrin releasing peptide receptor-positive tumors. *Nucl. Med. Biol*., **2002**, *29*, 553-60.

[16] Scopinaro, F.; Varvarigou, A.D.; Ussof, W.; De Vicentis, G.; Sourlingas, T.G.; Evangelatos, G.P. Technetium labeled bombesin-like peptide: preliminary report on breast cancer uptake in patients. *Cancer Biother. Radiopharm*., **2002**, *17*, 327-35.

[17] Scopinaro, F.; De Vicentis, G.; Varvarigou, A.D.; Laurenti, C.; Iori, F.; Remediani, S. ^{99m}Tc-bombesin detects prostate cancer and invasion of pelvic lymph nodes. *Eur. J. Nucl. Med. Mol. Imaging*, **2003**, *30*, 1378-82.

[18] Chen, X.; Park, R.; Hou, Y.; Tohme, M.; Shahinian, A.H.; Bading, J.R. microPET and autoradiographic imaging of GRP receptor expression with ^{64}Cu-DOTA-[Lys^3]bombesin in human prostate adenocarcinoma xenografts. *J. Nucl. Med.* **2004**, *45*, 1390-97.

[19] Alves, S.; Correia, J.D.; Santos, I.; Veerendra, B.; Sieckman, G.L.; Hoffman, T.J.; Rold, T.L.; Figueroa, S.D.; Retzloff, L.; McCrate, J.; Prasanphanich, A.; Smith, C.J. Pyrazolyl conjugates of bombesin: a new tridentate ligand framework for the stabilization of fac-[M(CO)3]+ moiety. *Nucl. Med. Biol.*, **2006**, *33*, 625-34.

[20] Ferro-Flores, G.; Arteaga de Murphy, C.; Rodriguez-Cortes, J.; Pedraza-Lopez, M.; Ramirez-Iglesias, MT. Preparation and evaluation of ^{99m}Tc-EDDA/HYNIC-[Lys^3]-bombesin for imaging gastrin-releasing peptide receptor-positive tumours. *Nucl. Med. Commun*., **2006**, *27*, 371-76.

[21] Zhang, X; Cai, W.; Cao, F.; Schreibmann, E.; Wu, Y.; Wu, J.C.; Xing, L.; Chen, X. ^{18}F-labeled bombesin analogs for targeting GRP

receptor-expressing prostate cancer. *J. Nucl. Med.*, **2006**, *47*, 492-501.

[22] Kunstler, J.U.; Veerendra, B.; Figueroa, S.D.; Sieckman, G.L.; Rold, T.L.; Hoffman, T.J.; Smith, C.J.; Pietzsch, H.J. Organometallic (99m)Tc(III) '4 + 1' bombesin(7–14) conjugates: synthesis, radiolabeling, and in vitro/in vivo studies. *Bioconjug. Chem.*, **2007**, *18*, 1651-716.

[23] de Visser, M.; van Weerden, W.M.; de Ridder, C-M. Androgen-dependent expression of the gastrin-releasing peptide receptor in human prostate tumor xenografts. *J. Nucl. Med.*, **2007**, *48*, 88-93.

[24] Santos-Cuevas, C.L.; Ferro-Flores, G.; Arteaga de Murphy, C.; Pichardo-Romero, P. Targeted imaging of gastrin-releasing peptide receptors with ^{99m}Tc-EDDA/HYNIC-[Lys^3]-bombesin: biokinetics and dosimetry in women. *Nucl. Med. Commun.*, **2008**, *29*, 741-47.

[25] van de Wiele, C.; Phonteyne, P.; Pauwels, P. Gastrin-releasing peptide receptor imaging in human breast carcinoma versus immunohistochemistry. *J. Nucl. Med.*, **2008**, *49*, 260-64.

[26] Schroeder, R.P.J.; van Weerden, W.M.; Bangma, C.; Krenning, E.P.; de Jong, M. Peptide receptor imaging of prostate cancer with radiolabelled bombesin analogues. *Methods*, **2009,** *48*, 200-4.

[27] von Guggenberg, E.; Behe, M.; Behr, T.M.; Saurer, M.; Seppi, T.; Decristoforo, C. ^{99m}Tc-labeling and *in vitro* and *in vivo* evaluation of HYNIC- and (Nalpha-His)acetic acid-modified [D-Glu1]-minigastrin. *Bioconjug. Chem.*, **2004**, *15*, 864-71.

[28] Nock, B.A.; Maina, T.; Behe, M.; Nikolopoulou, A.; Gotthardt, M.; Schmitt, J.S.; Behr, T.M.; Macke, H.R. CCK-2/Gastrin receptor–targeted tumor imaging with ^{99m}Tc-labeled minigastrin analogs. *J. Nucl. Med.*, **2005**, *46*, 1727-36.

[29] Bhattacharya, R.; Mukherjee, P. Biological properties of "naked" metal nanoparticles. *Adv. Drug Deliv. Rev.*, **2008**, *60*, 1289-306.

[30] Haubner, R.; Wester, H.J.; Reuning, U. Radiolabelled alfa$_v$beta3 integrin antagonists: a new class of tracers for tumor targeting. *J. Nucl. Med.*, **1999**, *40*, 1061-71.

[31] Haubner, R.; Wester, H.J.; Burkhart, F. Glycosylated RGD-containing peptides: tracer for tumor targeting and angiogenesis imaging with improved biokinetics. *J. Nucl. Med.*, **2001**, *42*, 326-36.

[32] Haubner. R.; Kuhnast, B.; Mang, C. [18F]Galacto-RGD: synthesis, radiolabeling, metabolic stability, and radiation dose estimates. *Bioconjug. Chem.*, **2004**, *15*, 61-9.

[33] Haubner, R.; Wester, H.J.; Weber, W.A. Non-invasive imaging of αvβ3 integrin expression using 18F-labelled RGD-containing glycopeptide and positron emission tomography. *Cancer Res.*, **2001**, *61*, 1781-5.

[34] Morrison, M.S.; Ricketts, S.A.; Barnett, J.; Cuthbertson, A.; Tessier, J.; Wedge, S.R. Use of a Novel Arg-Gly-Asp Radioligand, 18F-AH111585, to determine changes in tumor vascularity after antitumor therapy. *J. Nucl. Med.*, **2009**, *50*, 116-22.

[35] Yoshimoto, M.; Ogawa, K.; Washiyama, K.; Shikano, N.; Mori, H.; Amano, R.; Kawai, K. alfa$_v$beta3 integrin-targeting radionuclide therapy and imaging with monomeric RGD peptide. *Int. J. Cancer*, **2008**, *123*, 709-715.

[36] Jeong, J.M.; Hong, M.K.; Chang, Y.S.; Lee, Y.S.; Kim, Y.J.; Cheon, G.J.; Lee, D.S.; Chung, J.K.; Lee, M.C. Preparation of a promising angiogenesis PET imaging agent: ^{68}Ga-labeled c(RGDyK)–isothiocyanatobenzyl-1,4,7-triazacyclononane-1,4,7-triacetic acid and feasibility studies in mice. *J. Nucl. Med.*, **2008**, *49*, 830-36.

[37] Li, Z.B.; Chen, K.; Chen, X. ^{68}Ga-labeled multimeric RGD peptides for microPET imaging of integrin αvβ3 expression. *Eur. J. Nucl. Med. Mol. Imaging*, **2008**, *35*, 1100-08.

[38] Kenny, L.M.; Coombes, R.C.; Oulie, I.; Contractor, K.B.; Miller, M.; Spinks, T.J.; McParland, B.; Cohen, P.S.; Hui, A.M.; Palmieri, C.; Osman, S.; Glaser, M.; Turton, D.; Al-Nahhas, A.; Aboagye, E.O. Phase I Trial of the positron-emitting arg-gly-asp (RGD) peptide radioligand ^{18}F-AH111585 in breast cancer patients. *J. Nucl. Med.*, **2008**, *49*, 879-86.

[39] Liu, Z.; Yan, Y.; Chin, F.T.; Wang, F.; Chen, X. Dual integrin and gastrin-releasing peptide receptor targeted tumor imaging using ^{18}F-labeled PEGylated RGD-bombesin heterodimer ^{18}F-FB-PEG3-Glu-RGD-BBN. *J. Med. Chem.*, **2009**, *52*, 425-32.

[40] Liu, Z.; Niu, G.; Wang, F.; Chen, X. (68)Ga-labeled NOTA-RGD-BBN peptide for dual integrin and GRPR-targeted tumor imaging. *Eur. J. Nucl. Med. Mol. Imaging*, **2009**, *36*, 1483-94.

[41] Haubner, R.; Decristoforo, C. Radiolabelled RGD peptides and peptidomimetics for tumour targeting. *Front. Biosci.*, **2009**, *14*, 872-86.

[42] Mitrasinovic, P.M. Advances in αvβ3 integrin-targeting cancer therapy and imaging with radiolabeled RGD peptides. *Curr. Radiopharm.*, **2009**, *2*, 214-19.

[43] Zaccaro, L.; Del Gatto, A.; Pedone, C.; Saviano, M. Peptides for tumour therapy and diagnosis: Current status and future directions. *Curr. Med. Chem.*, **2009**, *16*, 780-95.

[44] Buchegger, F.; Bonvin, F.; Kosinski, M.; Schaffland, A.O.; Prior, J.; Reubi, J.C.; Blauenstein, P.; Tourwe, P.; García-Garayoa, E.; Bischof A. Radiolabelled neurotensin analog, ^{99m}Tc-NT-XI, evaluated in ductal pancreatic adenocarcinoma patients. *J. Nucl. Med.*, **2003**, *44*, 1649-54.

[45] Korner, M.; Waser, B.; Reubi, J.C. High expression of neuropeptide Y1 receptors in Ewing sarcoma tumors. *Clin. Canc. Res.*, **2008**, *14*, 5043-49.

[46] Zwanziger, D.; Khan, I.U.; Neundorf, I. Novel chemically modified analogues of neuropeptide Y for tumor targeting. *Bioconjug. Chem.*, **2008**, *19*, 1430-38.

[47] Kersemans, V.; Kersemans, K.; Cornelissen, B. Cell penetrating peptides for *in vivo* molecular imaging applications. *Curr. Pharm. Des.*, **2008**, *14*, 2415-27.

[48] Deshayes, S.; Morris, M.C.; Divita, G.; Heitz, F. Interactions of primary amphipathic cell penetrating peptides with model membranes: consequences on the mechanisms of intracellular delivery of therapeutics. *Curr. Pharm. Des.*, **2005**, *11*, 3629-38.

[49] Cornelissen, B.; McLarty, K.; Kersemans, V.; Scollard, D.; Reilly, R. Properties of [^{111}In]-labeled HIV-1 tat peptide radioimmunoconjugates in tumor-bearing mice following intravenous or intratumoral injection. *Nucl. Med. Biol.*, **2008**, *35*, 101-10.

[50] Costantini, D.L.; Hu, M.; Reilly, R. Peptide motifs for insertion of radiolabeled biomolecules into cells and routing to the nucleus for cancer imaging or radiotherapeutic applications. *Cancer Biother. Radiopharm.*, **2008**, *23*, 3-23.

[51] Santos-Cuevas, C.L.; Ferro-Flores, G.; Arteaga de Murphy, C.A.; Ramírez, F. de M.; Luna-Gutiérrez, M.A.; Pedraza-López, M.; García-Becerra, R.; Ordaz-Rosado, D. Design, preparation, *in vitro* and *in vivo* evaluation of ^{99m}Tc-N_2S_2-Tat(49–57)-bombesin: a target-specific hybrid radiopharmaceutical. *Int. J. Pharm.*, **2009**, *375*, 75-83.

[52] Ntziachristos, V.; Bremer, C.; Weissleder, R. Fluorescence imaging with near-infrared light: new technological advances that enable *in vivo* molecular imaging. *Eur. Radiol.*, **2003**, *13*, 195-208.

[53] Frangioni, J. V. *In vivo* near-infrared fluorescence imaging. *Curr. Opin. Chem. Biol.*, **2003**, *7*, 626-34.

[54] Sharma, P.; Brown, S.; Walte, G.; Santra, S.; Moudgil, B. Nanoparticles for bioimaging. *Adv. Colloid Interface Sci.*, **2006**, *123*, 471-85.

[55] Weissleder, R. A clearer vision for *in vivo* imaging. *Nat. Biotechnol.*, **2001**, *19*, 316-7.

[56] Ntziachristos, V.; Schellenberger, E.A.; Ripoll, J.; Yessayan, D.; Graves, E.; Bogdanov, A. Visualization of antitumor treatment by means of fluorescence molecular tomography with an annexin V–Cy5.5 conjugate. *Proc. Natl. Acad. Sci. U.S.A.*, **2004**, *101*, 12294-99.

[57] Graves, E.E.; Culver, J.P.; Ripoll, J.; Weissleder, R.; Ntziachristos, V. Singular-value analysis and optimization of experimental parameters in fluorescence molecular tomography. *J. Opt. Soc. Am. A.*, **2004**, *21*, 231-41.

[58] Graves, E.E.; Yessayan, D.; Turner, G.; Weissleder, R.; Ntziachristos, V. Validation of *in vivo* fluorochrome concentrations measured using fluorescence molecular tomography. *J. Biomed. Opt.*, **2005**, *10*, 44019 (doi:10.1117/1.1993427).

[59] Graves, E.E.; Ripoll, J.; Weissleder, R.; Ntziachristos, V. A submillimeter resolution fluorescence molecular imaging system for small animal imaging. *Med. Phys.*, **2003**, *30*, 901-11.

[60] Graves, E.E.; Weissleder, R.; Ntziachristos, V. Fluorescence molecular imaging of small animal tumor models. *Curr. Mol. Med.*, **2004**, *4*, 419-30.

[61] Ntziachristos, V.; Bremer, C.; Tung, C.; Weissleder, R. Imaging cathepsin B up-regulation in HT-1080 tumor models using fluorescence-mediated molecular tomography (FMT). *Acad. Radiol.*, **2002**, *9*, S323-25.

[62] Ntziachristos, V.; Weissleder, R. Charge-coupled-device based scanner for tomography of fluorescent near-infrared probes in turbid media. *Med. Phys.*, **2002**, *29*, 803-9.

[63] Gao, M.; Lewis, G.; Turner, G.M.; Soubret, A.; Ntziachristos, V. Effects of background fluorescence in fluorescence molecular tomography. *Appl. Opt.*, **2005**, *44*, 5468-74.

[64] Gremlich, H.U.; Martinez, V.; Kneuer, R.; Kinzy, W.; Weber, E.; Pfannkuche, H.J. Non-invasive assessment of gastric emptying by near-infrared fluorescence reflectance imaging in mice: pharmacological validation with tegaserod, cisapride, and clonidine. *Mol. Imaging*, **2004**, *3*, 303-11.

[65] Tung, C.H.; Quinti, L.; Jaffer, F.A.; Weissleder, R. A branched fluorescent peptide probe for imaging of activated platelets. *Mol. Pharm.*, **2005**, *2*, 92-5.

[66] Ntziachristos, V.; Bremer, C.; Graves, E.E.; Ripoll, J.; Weissleder, R. *In vivo* tomographic imaging of near-infrared fluorescent probes. *Mol. Imaging*, **2002**, *1*, 82-88.

[67] Cai, W.; Chen, X. Preparation of peptide-conjugated quantum dots for tumor vasculature-targeted imaging. *Nat. Prot.*, **2008,** *3*, 89-96.

[68] Lyons, A.B.; Parish, C.R. Determination of lymphocyte division by flow cytometry. *J. Immunol. Methods*, **1994**, *171*, 131-7.

[69] Lin, Y.; Weissleder, R.; Tung, C.H. Synthesis and properties of sulfhydryl-reactive near-infrared cyanine fluorochromes for fluorescence imaging. *Mol. Imaging*, **2003**, *2*, 87-92.

[70] Licha, K.; Riefke, B.; Ntziachristos, V.; Becker, A.; Chance, B.; Semmler, W. Hydrophilic cyanine dyes as contrast agents for near-infrared tumor imaging: synthesis, photophysical properties and spectroscopic *in vivo* characterization. *Photochem. Photobiol.*, **2000**, *72*, 392-98.

[71] Pham, W.; Lai, W.F.; Weissleder, R.; Tung, C.H. High efficiency synthesis of a bioconjugatable near-infrared fluorochrome. *Bioconjug. Chem.*, **2003**, *14*, 1048-51.

[72] Frangioni, J.V. *In vivo* near-infrared fluorescence imaging. *Curr. Opin. Chem. Biol*., **2003**, *7*, 626-34.

[73] Kim, S.; Lim, Y.T.; Soltesz, E.G.; Lee, J.; Nakayama, A. Near-infrared fluorescent type II quantum dots for sentinel lymph node mapping. *Nat. Biotechnol.*, **2004**, *22*, 93-97.

[74] Kojima, H. Development of near-infrared fluorescent probes for *in vivo* imaging. *Yakugaku Zasshi*, **2008**, *128*, 1653-63.

[75] Chen, X.; Conti, P.S.; Moats, R.A. *In vivo* near-infrared fluorescence imaging of integrin αvβ3 in brain tumor xenografts. *Cancer Res.*, **2004**, *64*, 8009-14.

[76] Cheng, Z.; Wu, Y.; Xiong, Z.; Gambhir, S.S.; Chen, X. Near-infrared fluorescent RGD peptides for optical imaging of integrin αvβ3 expression in living mice. *Bioconjug. Chem.*, **2005**, *16*, 1433-41.

[77] Hsu, A.R.; Hou, L.C.; Veeravagu, A.; Greve, J.M.; Vogel, H.; Tse, V.; Chen, X. *In vivo* near-infrared fluorescence imaging of integrin αvβ3 in an orthotopic glioblastoma model. *Mol. Imaging Biol.*, **2006**, *8*, 315.

[78] Wang, W.; Ke, S.; Wu, Q.; Charnsangavej, C.; Gurfinkel, M.; Gelovani, J.G.; Abbruzzese, J.L.; Sevick-Muraca, E.M.; Li, C. Near-infrared optical imaging of integrin alphavbeta3 in human tumor xenografts. *Mol. Imaging*, **2004**, *3*, 343-51.

[79] Gurfinkel, M.; Ke, S.; Wang, W.; Li, C.; Sevick-Muraca, E.M. Quantifying molecular specificity of αvβ3 integrin-targeted optical contrast agents with dynamic optical imaging. *J. Biomed. Opt.*, **2005**, *10*, 34019 (doi:10.1117/1.1924696).

[80] Wu, Y.; Cai, W.; Chen, X. Near-infrared fluorescence imaging of tumor integrin αvβ3 expression with Cy7-labeled RGD multimers. *Mol. Imaging Biol.*, **2006**, *8*, 226-36.

[81] Waldeck, J.; Häger, F.; Höltke, C.; Lanckohr, C.; Wallbrunn, A.; Torsello, G.; Heindel, W.; Theilmeier, G.; Schäfers, M.; Bremer, C. Fluorescence reflectance imaging of macrophage-rich atherosclerotic plaques using an αvβ3 integrin–targeted fluorochrome. *J. Nucl. Med.*, **2008**, *49*, 1845-51.

[82] Achilefu, S.; Bloch, S.; Markiewicz, M. A.; Zhong, T. X.; Ye, Y. P.; Dorshow, R. B.; Chance, B.; Liang, K. X. Synergistic effects of light-emitting probes and peptides for targeting and monitoring integrin expression. *Proc. Natl. Acad. Sci. U.S.A.*, **2005**, *102*, 7976-81.

[83] Bloch, S.; Liang, K.; Dorshow, R. B.; Ye, Y.; Achilefu, S. Targeting the expression of integrin receptors in tumors. *Proc. SPIE*, **2004**, *5329*, 222 (doi:10.1117/12.533160).

[84] Ye, Y.; Bloch, S.; Xu, B.; Achilefu, S. Design, synthesis, and evaluation of near infrared fluorescent multimeric RGD peptides for targeting tumors. *J. Med. Chem.*, **2006**, *49*, 2268-75.

[85] Wu, P.; He, X.; Wang, K.; Tan, W.; Ma, D.; Yang, W.; He, C. Imaging breast cancer cells and tissues using peptide-labeled fluorescent silica nanoparticles. *J. Nanosci. Nanotechnol.*, **2008**, *8*, 2483-7.

[86] Ma. L.; Yu, P.; Veerendra, B.; Rold, T.L.; Retzloff, L.; Prasanphanich, A.; Sieckman, G.; Hoffman, T.J.; Volkert, W.A.; Smith, C.J. *In vitro* and *in vivo* evaluation of alexa fluor 680-Bombesin[7-14]NH_2 peptide conjugate, a high-affinity fluorescent probe with high selectivity for the gastrin-releasing peptide receptor. *Mol. Imaging*, **2007,** *6*, 171-80.

[87] Chan, W.C.W.; Maxwell, D.J.; Gao, X.H.; Bailey, R.E.; Han, M.Y.; Nie, S.M. Luminescent quantum dots for multiplexed biological detection and imaging. *Curr. Opin. Biotechnol.*, **2002**, *13*, 40-46.

[88] Han, M.Y.; Gao, X.H.; Su, J.Z.; Nie, S.M. Quantum dot-tagged microbeads for multiplexed optical coding of biomolecules. *Nat. Biotechnol.*, **2001**, *19*, 631-35.

[89] Gao, X.H.; Nie, S.M. Doping mesoporous materials with multicolor quantum. *J. Phys. Chem. B*, **2003**, *107*, 11575-78.

[90] Gao, X.H.; Nie, S.M. Quantum dot-encoded mesoporous beads with high brightness and uniformity: rapid readout using flow cytometry. *Anal. Chem.*, **2004**, *76*, 2406-10.

[91] Gao, X.H.; Yang, L.; Petros, J.A.; Marshall, F.M.; Simons, J.W.; Nie1, S. *In vivo* molecular and cellular imaging with quantum dots. *Curr. Opin. Biotechnol.*, **2005**, *16*, 63-72.

[92] Manna, L.; Milliron, D.J.; Meisel, A.; Scher, E.C.; Alivisatos, A.P. Controlled growth of tetrapod-branched inorganic nanocrystals. *Nat. Mater.*, **2003**, *2*, 382-85.

[93] Milliron, D.J.; Hughes, S.M.; Cui, Y.; Manna, L.; Li, J.; Wang, L.W.; Alivisatos, A.P. Colloidal nanocrystal heterostructures with linear and branched topology. *Nature*, **2004**, *430*, 190-5.

[94] Dick, K.A.; Deppert, K.; Larsson, M.W.; Martensson, T.; Seifert, W.; Wallenberg, L.R.; Samuelson, L. Synthesis of branched 'nanotrees' by controlled seeding of multiple branching events. *Nat. Mater.*, **2004,** *3*, 380-84.

[95] Yu, W.W.; Wang, Y.A.; Peng, X.G. Formation and stability of size-, shape-, and structure-sontrolled CdTe nanocrystals: ligand effects on monomers and nanocrystals. *Chem. Mater.*, **2003**, *15*, 4300-8.

[96] Hines, M.A.; Guyot-Sionnest, P. Synthesis and characterization of strongly luminescing ZnS-capped CdSe nanocrystals. *J. Phys. Chem. B*, **1996**, *100*, 468-71.

[97] Peng, X.G.; Schlamp, M.C.; Kadavanich, A.V.; Alivisatos, A.P. Epitaxial growth of highly luminescent CdSe/CdS core/shell nanocrystals with photostability and electronic accessibility. *J. Am. Chem. Soc.*, **1997**, *119*, 7019-29.

[98] Dabbousi, B.O.; Rodriguez-Viejo, J.; Mikulec, F.V.; Heine, J.R.; Mattoussi, H.; Ober, R.; Jensen, K.F.; Bawendi, M.G. (CdSe)ZnS core−shell quantum dots: synthesis and characterization of a size series of highly luminescent nanocrystallites. *J. Phys. Chem. B*, **1997**, *101*, 9463-75.

[99] Bailey, R.E.; Nie, S. Alloyed semiconductor quantum dots: tuning the optical properties without changing the particle size. *J. Am. Chem. Soc.*, **2003**, *125*, 7100-6.

[100] Gao, X.H.; Cui, Y.Y.; Levenson, R.M.; Chung, L.W.K.; Nie, S.M. *In vivo* cancer targeting and imaging with semiconductor quantum dots. *Nat. Biotechnol.*, **2004**, *22*, 969-76.

[101] Smith, A.; Duan, H.; Mohs, A.M.; Nie, S. Bioconjugated quantum dots for *in vivo* molecular and cellular imaging. *Adv. Drug Deliv. Rev.*, **2008**, *60*, 1226-40.

[102] Medintz, I.L.; Clapp, A.R.; Mattoussi, H.; Goldman, E.R.; Fisher, B.; Mauro, J.M. Self-assembled nanoscale biosensors based on quantum dot FRET donors. *Nat. Mater.*, **2003**, *2*, 630-8.

[103] Shah, B.S.; Clark, P.A.; Moioli, E.K.; Stroscio, M.A.; Mao, J.J. Labeling of mesenchymal stem cells by bioconjugated quantum dots. *Nano Lett.*, **2007**, *7*, 3071-79.

[104] Young, S.H.; Rozengurt, E. Qdot nanocrystal conjugated to bombesin or ANG II label the cognate G protein-coupled receptor in living cells. *Am. J. Physiol. Cell Physiol.*, **2006**, *290*, C728-32.

[105] Chen, F.; Gerion, D. Fluorescent CdSe/ZnS nanocrystal−peptide conjugates for long-term, nontoxic imaging and nuclear targeting in living cells. *Nano Lett.*, **2004**, *4*, 1827-32.

[106] Ruan, G.; Agrawal, A.; Marcus, A.I.; Nie, S.M. Imaging and tracking of tat peptide-conjugated quantum dots in living cells: new

insights into nanoparticle uptake, intracellular transport, and vesicle shedding. *J. Am. Chem. Soc.*, **2007**, *129*, 14759-66.

[107] Wadia, J.S.; Dowdy, S.F. Transmembrane delivery of protein and peptide drugs by TAT-mediated transduction in the treatment of cancer. *Adv. Drug Deliv. Rev.*, **2005**, *57*, 579-96.

[108] Gonczy, P.; Pichler, S.; Kirkham, M.; Hyman, A.A. Cytoplasmic dynein is required for distinct aspects of Mtoc positioning, including centrosome separation, in the one cell stage caenorhabditis elegans embryo. *J. Cell Biol.*, **1999**, *147*, 135-50.

[109] Liu, Z.; Cai, W.; He, L,; Nakayama, N.; Chen, K.; Sun, X.; Chen, X.; Dai, H. *In vivo* biodistribution and highly efficient tumour targeting of carbon nanotubes in mice. *Nat. Nanotechnol.*, **2007**, *2*, 47-52.

[110] De La Zerda, A.; Zavaleta, C.; Keren, S.; Vaithilingam, S.; Bodapati, S.; Liu, Z.; Levi, J.; Smith, B.R.; Ma, T.; Oralkan, O.; Cheng, Z.; Chen, X.; Dai, H.; Khuri-Yakub, B.T.; Gambhir, S.S. Carbon nanotubes as photoacoustic molecular imaging agents in living mice. *Nat. Nanotechnol.*, **2008**, *3*, 557-62.

[111] Connor, E.E.; Mwamuka, J.; Gole, A.; Murphy, C.J.; Wyatt, M. Gold nanoparticles are taken up by human cells but do not cause acute cytotoxicity. *Small*, **2005**, *1*, 325-7.

[112] Brust, M.; Fink, J.; Bethell, D.; Schiffrin, D.J.; Kiely, C. Synthesis and reactions of functionalised gold nanoparticles. *J. Chem. Soc. Chem. Commun.*, **1995**, *16*, 1655-56.

[113] Pissuwan, D.; Valenzuela, S.M.; Cortie, M.B. Therapeutic possibilities of plasmonically heated gold nanoparticles. *Trends Biothecnol.*, **2006**, *24*, 62-67.

[114] Chompoosor, A.; Han, G.; Rotello, V.R. Charge dependence of ligand release and monolayer stability of gold nanoparticles by biogenic thiols. *Bioconjug. Chem.*, **2007**, *19*, 1342-5.

[115] Surujpaul, P.P.; Gutierrez-Wing, C.; Ocampo-Garcia, B.; Ramirez, F. de M.; Arteaga de Murphy, C.; Pedraza-Lopez, M.; Camacho-Lopez, M.A.; Ferro-Flores, G. Gold nanoparticles conjugated to [Tyr^3]octreotide peptide. *Biophys. Chem.*, **2008**, *138*, 83-90.

[116] De la Fuente, J.M.; Berry, C.C. Tat Peptide as an efficient molecule to translocate gold nanoparticles into the cell nucleus. *Bioconjug. Chem.*, **2005**, *16*, 1176-80.

[117] De la Fuente, J.M.; Berry, C.C.; Riehle, M.O.; Curtis, S.G. NPs targeting at cells. *Langmuir*, **2006**, *22*, 3286-93.

[118] Montet, X.; Montet-Abou, K.; Reynolds, F.; Weissleder, R.; Josephson, L. Nanoparticle imaging of integrins on tumor cells. *Neoplasia*, **2006**, *8*, 214-22.

[119] Sun, S.H.; Zeng, H.; Robinson, D.B.; Raoux, S.; Rice, P.M.; Wang, S.X.; Li, G.X. Monodisperse MFe_2O_4 (M = Fe, Co, Mn) Nanoparticles. *J. Am. Chem. Soc.*, **2004**, *126*, 273-9.

[120] Lee, J.H.; Huh, Y.M.; Jun, Y.W.; Seo, J.W.; Jang, J.T.; Song, H.T.; Kim, S.; Cho, E.J.; Yoon, H.G.; Suh, J.S.; Cheon, J. Artificially engineered magnetic nanoparticles for ultra-sensitive molecular imaging. *Nat. Med.*, **2007**, *13*, 95-99.

[121] Xu, C.J.; Sun, S.H. Monodisperse magnetic nanoparticles for biomedical applications. *Polym. Int.*, **2007**,*56*, 821-26.

[122] Baldi, G.; Bonacchi, D.; Franchini, M.C.; Gentili, D.; Lorenzi, G.; Ricci, A.; Ravagli, C. Synthesis and coating of cobalt ferrite nanoparticles: a first step toward the obtainment of new magnetic nanocarriers. *Langmuir*, **2007**, *23*, 4026-8.

[123] Peng, S.; Wang, C.; Xie, J.; Sun, S. Synthesis and stabilization of monodisperse Fe nanoparticles. *J. Am. Chem. Soc.*, **2006**, *128*, 10676-77.

[124] Qiang, Y.; Antony, J.; Sharma, A.; Nutting, J.; Sikes, D.; Meyer, D. Iron/iron oxide core-shell nanoclusters for biomedical applications. *J. Nanopart. Res.*, **2006**, *8*, 489-96.

[125] Sun, S.H. Recent advances in chemical synthesis, self-assembly, and applications of FePt nanoparticles. *Adv. Mater.*, **2006**, *18*, 393-403.

[126] Kogan, M.J.; Olmedo, I.; Hosta, L.; Guerrero, A.R.; Cruz, L.J.; Albericio, F. Peptides and metallic nanoparticles for biomedical applications. *Nanomedicine*, **2007**, *2*, 287-306.

[127] Berry, C.C.; Curtis, S.G. Functionalisation of magnetic nanoparticles for applications in biomedicine. *J. Phys. D Appl. Phys.*, **2003**, *36*, R198-206.

[128] Montet, X.; Weissleder, R.; Josephson, L. Imaging pancreatic cancer with a peptide-nanoparticle conjugate targeted to normal pancreas. *Bioconjug. Chem.*, **2006**, *17*, 905-11.

[129] Zhao, M.; Kircher, M.F.; Josephson, L.; Weissleder, R. Differential Conjugation of Tat Peptide to Superparamagnetic Nanoparticles and Its Effect on Cellular Uptake. *Bioconjug. Chem.*, **2002**, *13*, 840-4.

[130] Garden, O.A.; Reynolds, P.R.; Yates, J. A rapid method for labelling CD4+ T cells with ultra small paramagnetic iron oxide NPs for magnetic resonance imaging that preserves proliferative, regulatory and migratory behaviour *in vitro*. *J. Inmunol. Methods*, **2006**, *314*, 123-33.

[131] Josephson, L.; Tung, C.H.; Moore, A.; Weissleder, R. High-efficiency intracellular magnetic labelling with novel superpara-magnetic–Tat peptide conjugates. *Bioconjug. Chem.*, **1999**, *10*, 186-91.

[132] Dodd, C.H., Hsu, H.C.; Chu, W.J. Normal T cell response and *in vivo* magnetic resonance imaging of T cells loaded with HIV transactivator-peptide-derived superparamagnetic NPs. *J. Immunol. Methods*, **2001**, *256*, 89-105.

[133] Lee, S.J.; Jeong, J.R.; Shin, S.C.; Huh Y.M.; Song, H.T.; Suh, J.S.; Chang, Y.H.; Jeon, B.S.; Kim, J.D. Intracellular translocation of superparamagnetic iron oxide NPs encapsulated with peptide conjugated poly(D,L lactide-co-glycolide). *J. Appl. Phys.*, **2005**, *97*, 10Q913 (Online Publication).

[134] O´Connor, M.K.; Kemp, B.J. Single-photon emission computed tomography/ computed tomography: basic instrumentation and innovations. *Semin. Nucl. Med.*, **2006,** *36*, 258-66.

[135] Delbeke, D.; Coleman, R.E.; Guiberteau, M.J.; Brown, M.L.; Royal, H.D.; Siegel, B.A. Procedure guideline for SPECT/CT Imaging. *J. Nucl. Med.*, **2006**, *47*, 1227-34.

[136] Cai, W.; Chen, K.; Li, Z.B.; Gambhir, S.S.; Chen, X. Dual-Function Probe for PET and Near-Infrared Fluorescence Imaging of Tumor Vasculature. *J. Nucl. Med.*, **2007**, *48*, 1862-70.

[137] McCann, C.M.; Waterman, P.; Figueiredo, J.L.; Aikawa, E.; Weissleder, R.; Chen, J.W. Combined magnetic resonance and fluorescence imaging of the living mouse brain reveals glioma response to chemotherapy. *Neuroimage*, **2009**, *45*, 360-9.

[138] Devaraj, N.K.; Keliher, E.J.; Thurber, G.M.; Nahrendorf, M.; Weissleder, R. F Labeled nanoparticles for *in vivo* PET-CT imaging. *Bioconjug. Chem.*, **2009**, *20*, 397-401.

[139] Bhushan, K.R.; Misra, P.; Liu, F.; Mathur, S.; Lenkinski, R.E.; Frangioni, J.V. Detection of breast cancer microcalcifications using a dual-modality SPECT/NIR fluorescent probe. *J. Am. Chem. Soc.*, **2008**, *130*, 17648-49.

Received: August 25, 2009 Revised: November 16, 2009 Accepted: November 16, 2009